# Various Sources of Wing Rock

L. E. Ericsson*
*Lockheed Missiles & Space Company, Inc., Sunnyvale, California*

**Limit cycle oscillations in roll of advanced aircraft can result from three different fluid mechanical flow processes. The so-called slender wing rock is caused by asymmetric vortex shedding from highly swept wing leading edges. A completely different flow mechanism causes wing rock for aircraft with moderately swept leading edges. In this case, the causative mechanism is dynamic airfoil stall. Finally, if the aircraft has a slender forebody, the rocking motion can be generated by asymmetric body vortices from the nose, which interact with a nonaxisymmetric aft body, e.g., due to the presence of wing or tail surfaces. This paper describes the nonsteady fluid dynamic processes generating the different types of wing rock.**

## Nomenclature

$b$ = wing span
$C_{\ell_p}$ = $(\partial C_\ell/\partial(pb/2U_\infty)$
$c$ = reference length, mean chord for wing body, maximum diameter $d$ for body alone
$d$ = cylinder diameter
$f$ = frequency of oscillation
$\ell$ = rolling moment coefficient $C_\ell = \ell/(\rho_\infty U_\infty{}^2/2)Sb$
$M$ = Mach number
$M_p$ = pitching moment: coefficient $C_m = M_p/(\rho_\infty U_\infty{}^2/2)Sc$
$N$ = normal force: coefficient $C_N = N/(\rho_\infty U_\infty{}^2/2)S$
$n$ = yawing moment: coefficient $C_n = n/(\rho_\infty U_\infty{}^2/2)Sb$
$p$ = spin rate
$q$ = pitch rate
$Re$ = Reynolds number, $Re = U_\infty d/\nu_\infty$
$S$ = reference area, wing area, or maximum cross-sectional area
$t$ = time
$U$ = velocity
$x$ = distance from nose tip or apex
$Y$ = side force: coefficient $C_Y = Y/(\rho_\infty U_\infty{}^2/2)S$; $c_y = \partial C_Y/\partial(x/d)$
$\dot{z}$ = $\partial z/\partial t$
$\alpha$ = angle of attack
$\beta$ = angle of sideslip
$\Delta$ = increment or amplitude
$\theta_A$ = apex half angle
$\Lambda$ = leading-edge sweep
$\nu$ = kinematic viscosity of air
$\rho$ = air density
$\phi$ = roll angle
$\omega$ = angular frequency, $\omega = 2\pi f$
$\bar{\omega}$ = reduced frequency, $\bar{\omega} = \omega c/U_\infty$

*Subscripts*

$A$ = apex half angle
$d$ = discontinuity
$F$ = flare
$N$ = nose tip
$W$ = wall
WR = wing rock
0 = initial or time-average value
$\infty$ = freestream conditions

*Superscripts*

$\bar{}$ = effective value, e.g., $\bar{\theta}_A$

## Introduction

PRESENT day high-performance aerospace vehicles are subject to unsteady flowfields that generate highly nonlinear aerodynamics with strong coupling between longitudinal and lateral degrees of freedom.[1-3] The complex vehicle dynamics are caused by separated flow effects of various types and can, therefore, usually not be predicted by theoretical means. As a consequence, heavy reliance has to be placed on phenomenological analyses, based on classic fluid mechanics and guided by flight data and dynamic subscale tests[4] where dynamic support interference[5] and dynamic simulation problems[6] add to the difficulty of determining the full-scale separated flow characteristics. In the present paper, existing experimental results for nonlinear pitch-yaw-roll coupling phenomena of high performance aircraft are analyzed to obtain an understanding of the basic fluid mechanics causing wing and body rock.

For convenience of exposition, the phenomena are discussed as several distinct cases involving the effects of boundary-layer separation, effective wing-sweep angle and angle of attack, body and vortex motions, vortex asymmetry, and burst. These distinctions are not clearly defined in nature, and it is understood that the phenomena are elements of a continuous spectrum. However, it is hoped that the discussions will permit a clearer understanding of wing rock across this spectrum as well as in the specific examples discussed.

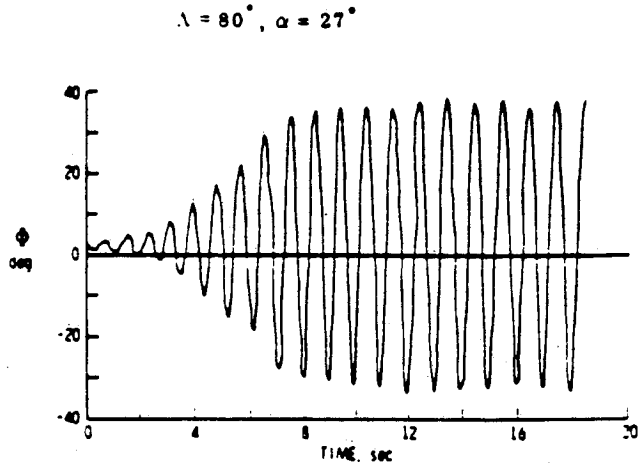


**Fig. 1 Wing-rock amplitude buildup at $\alpha = 27$ deg for an 80-deg delta wing (see Ref. 7), $\Lambda = 80$ deg.**

Received Feb. 11, 1989; revision received Dec. 12, 1989. 

*Senior Consulting Engineer. Fellow AIAA.

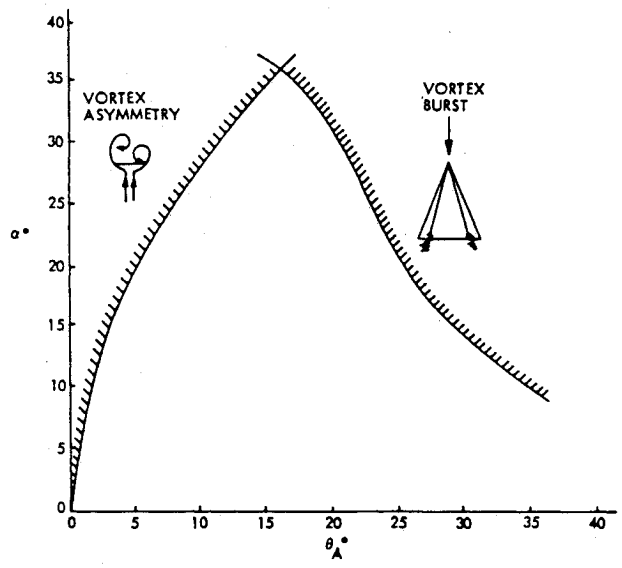


Fig. 2 Boundaries for vortex asymmetry and vortex burst (see Ref. 10).

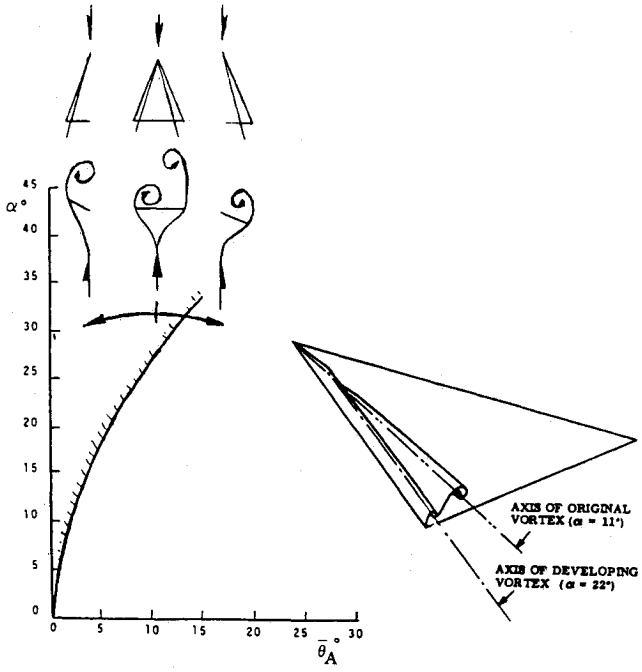


Fig. 3 Wing rock caused by asymmetric leading-edge vortices.

## Discussion

The different flow phenomena, as they can be deduced from available experimental results, will be described, starting with the case of slender wing rock.

## Slender Wing Rock

Systematic experiments performed by Nguyen, Yip, and Chambers[7] provided the information needed to fully describe the fluid mechanic phenomenon leading to slender wing rock.[8] The phenomenon is similar in many aspects to the limit cycle oscillation in pitch observed on blunt cylinder-flare bodies.[9] Thus, the roll oscillations of an 80-deg delta wing are self-excited and build up to a limit cycle amplitude[7] (see Fig. 1).

It is shown in Ref. 8 that the causative flow mechanism is asymmetry of the leading-edge vortices, which has been observed to occur before vortex burst when the leading-edge sweep $\Lambda$ deg = 90 deg $- \theta_A$ deg is larger than 74 deg[10] (see Fig. 2). Figure 3 illustrates the fluid mechanical reasons for this. At an $\alpha, \theta_A$ combination where vortex asymmetry occurs, the wing half with the lifted-off vortex loses lift and "dips down," rotating around the roll axis. As a result of the increasing roll angle, the effective apex half angle $\theta_A$ is increased, and the vortex attaches again. (The reformation of the vortex will also be influenced by the roll-motion-induced angle of attack.) This produces a restoring rolling moment, the positive aerodynamic spring needed for the rigid-body oscillation in roll (see Fig. 1). Due to the convective time lag[11] (see inset in Fig. 3), the statically stabilizing vortex-induced rolling moment is dynamically destabilizing.[8] Thus, the roll amplitude increases until the amplitude has reached its limit-cycle magnitude, at which the dynamically destabilizing effect is balanced by the damping from the attached vortex or vortices on both sides of the roll angle $\phi_d$, where the discontinuous change of the vortex-induced lift and associated rolling moment occurs.

Thus, the discontinuity introduced by the vortex asymmetry has all the characteristics needed to generate the observed limit cycle oscillation in roll, whereas vortex breakdown is lacking these characteristics, as is discussed in Ref. 8. In fact, it is shown in Ref. 12 that vortex burst is the flow mechanism limiting the growth of the slender wing-rock amplitude with increasing angle of attack. As the vortex burst jumps far for-

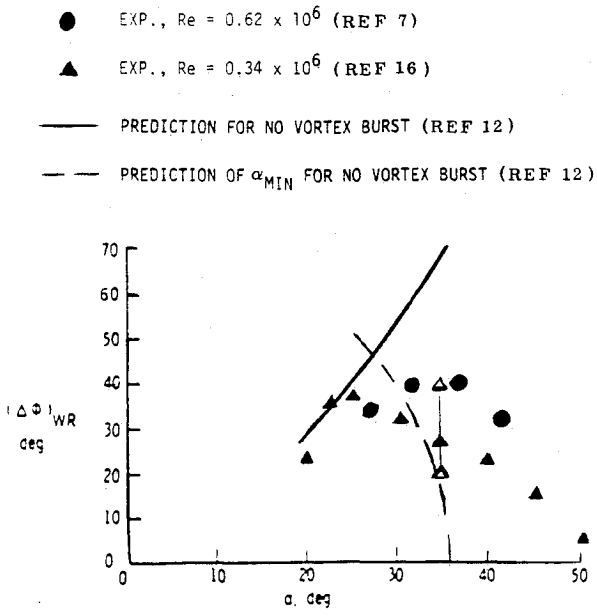


Fig. 4 Comparison between predicted and measured wing-rock amplitudes (see Ref. 12).

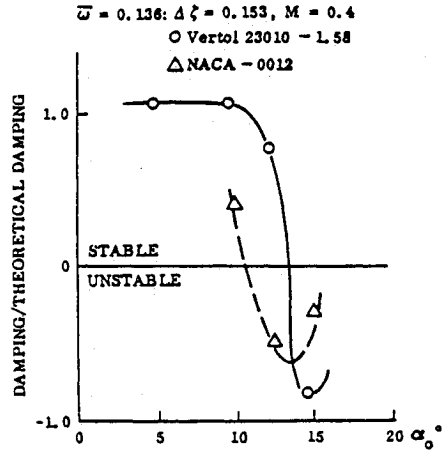


Fig. 5 Damping characteristics for airfoils in plunging oscillations (see Ref. 17).

ward of the trailing edge when it starts occurring for the sweep angles of interest, $\Lambda > 70$ deg,[13] the associated loss of suction lift effectively stops the trend of increasing wing rock amplitude with increasing angle of attack[12] (see Fig. 4). Existing numerical prediction methods[14,15] have not yet been developed to the point where they can handle vortex burst.

Slender wing rock, in spite of all the attention it has received, will rarely be the source of wing rock on present and future advanced aircraft. It can occur only on flying-wing type of configurations and possibly also to a limited extent on blended wing-body forebodies. If the wing is preceded by a slender forebody, as is mostly the case, the vortex-asymmetry is generated by the forebody, not by interacting leading-edge vortices, as in the case of slender wing rock. Although the asymmetric vortices need to interact with downstream wing and/or tail surfaces in order to generate wing rock, the source of the wing rock is asymmetric forebody flow separation, not asymmetry of the leading-edge vortices from a slender wing.

## Conventional Wing Rock

The flow mechanism causing wing rock of straight or moderately swept wings is closely related to dynamic stall. The experimental results[17] in Fig. 5 show that plunging oscillations of an airfoil are undamped in the stall region. It is the "leading-edge jet," the moving wall/wall jet analogy discussed in Ref. 18 (see Fig. 6), that produces the negative aerodynamic damping in plunge[19] shown in Fig. 5. If an aircraft is perturbed when flying close to stall, the downrolling wing half will experience the upstream moving wall effect illustrated for the downstroke in Fig. 6. As it promotes separation, the loss of lift is increased beyond the static lift loss, more the higher the plunging rate is. This generates a rolling moment that drives the motion; i.e., it is undamping. The delayed stall due to downstream moving wall effects on the opposite wing (upstroke in Fig. 6) generates positive lift that adds to the undamping rolling moment.

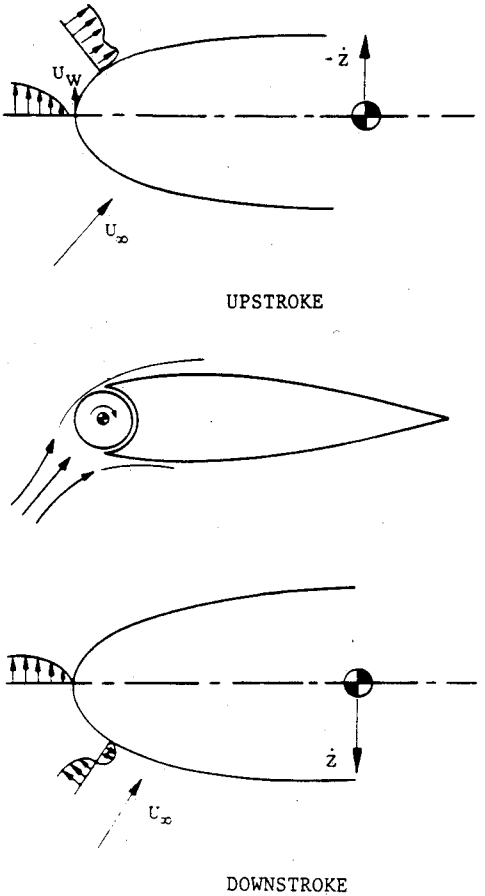


Fig. 6 Leading-edge jet effect (see Ref. 18).

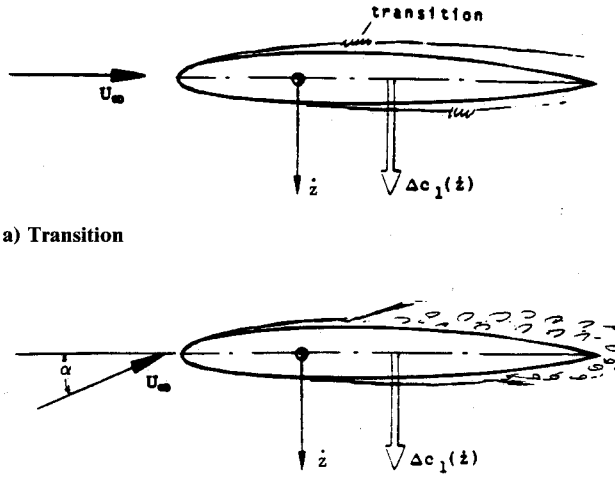


Fig. 7 Transition and flow separation characteristics for plunging oscillations.

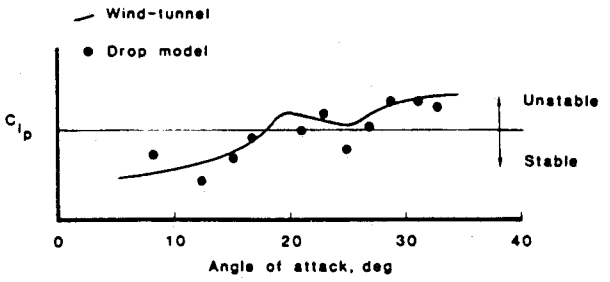


Fig. 8 Roll-damping characteristics of the X-29A models (see Ref. 23).

Thus, the induced effects of the local plunging velocity $\dot{z}$ drive the wing in roll. What stops the rolling motion to produce wing rock? Figure 5 gives the answer. When the roll angle has been increased enough to cause $\alpha_{EFF}$ to decrease below $\alpha_{STALL}$ on the downgoing wing half, the flow will reattach. This generates the lift needed to produce a restoring rolling moment. This is the aerodynamic spring needed for wing rock, as was described earlier, that produces the (positive) damping needed to balance the negative damping (undamping) generated at lower roll angles with associated higher $\alpha_{EFF}$ (see Fig. 5).

Boundary-layer transition can by itself have a significant effect, causing divergent wing bending oscillations.[20,21] The plunging airfoil section for the bending wing will experience a transition-promoting moving wall effect on the top side during the down stroke of the bending oscillation. On the bottom side, the moving wall effect is the opposite, delaying transition. As a result, a negative lift component is generated, which drives the oscillation (see Fig. 7a). How this coupling of transition to the bending oscillation via the moving wall effect can generate the observed bending oscillation[20] is described in Ref. 21, where it is also shown that the flat-top pressure distribution typical of advanced airfoils[22] make them especially susceptible to transition-induced bending oscillations. Figure 7b illustrates how the plunging-induced moving wall effect would generate a similar negative force component in the case of laminar separation. The same is also the case for "purely" turbulent separation, although transition will have some effect.[21]

In the present case of interest, the negative lift component in Fig. 7 will, of course, produce wing rock rather than wing

bending oscillations. Negative roll damping, leading to wing rock, has been observed for the X-29A aircraft[23] both in the wind tunnel (see Fig. 8) and in drop tests[23] (see Fig. 9). For the low aspect-ratio wing, stall would occur somewhere around $\alpha = 20$ deg. A roll damper was found to eliminate this classic wing rock but not the one caused by forebody vortices (see Fig. 9). (Courtesy of the authors of Ref. 23. This figure was shown in the oral presentation at the AIAA Atmospheric Flight Mechanics Conference, Monterey, California, Aug. 17–19, 1987, but is not contained in Ref. 23.)

## Wing-Body Rock

Recent experimental results[24] (see Fig. 10) indicate that the wing rock induced by forebody vortices is more violent than the one induced by the leading-edge vortices on a slender ($\Lambda = 80$ deg) delta wing[7] (see Fig. 1), with the buildup to the 30- to 40-deg limit cycle amplitude occurring over less than 3 cycles rather than approximately 10. Flow visualization pictures taken during the wing-rock show, according to the authors,[24] the same type of asymmetry switching of the vortices as for the slender delta wing.[7] Based on the observed sensitivity to forebody geometry of the asymmetric vortex phenomenon,[25,26] a number of forebody geometries were tested.[24] The results were rather surprising.[7] Only the chine configuration showed a significant change of the wing-rock amplitude

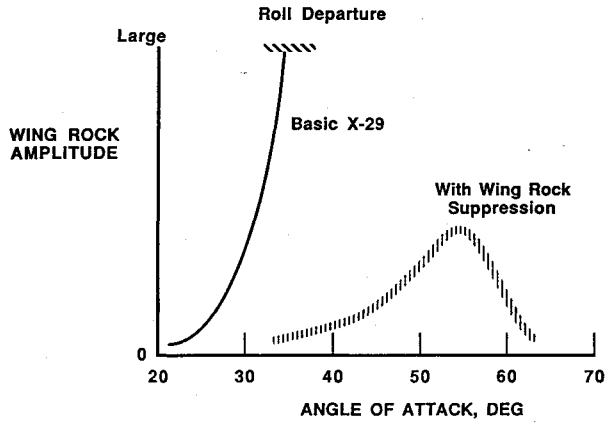


**Fig. 9 Wing-rock characteristics of the X-29A (see Ref. 23).**

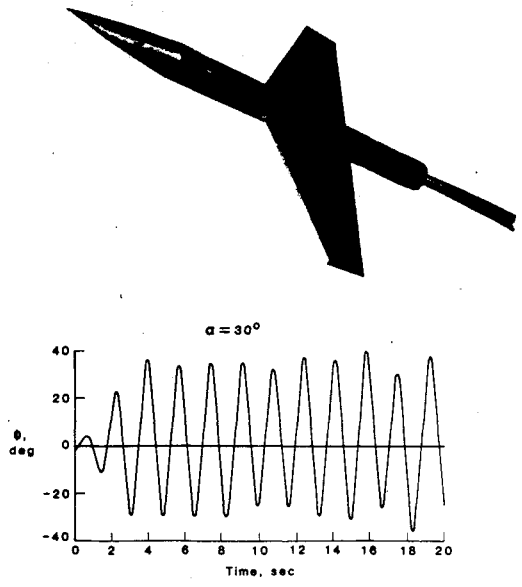


**Fig. 10 Wing rock buildup at $\alpha = 30$ deg for generic aircraft model (see Ref. 24).**

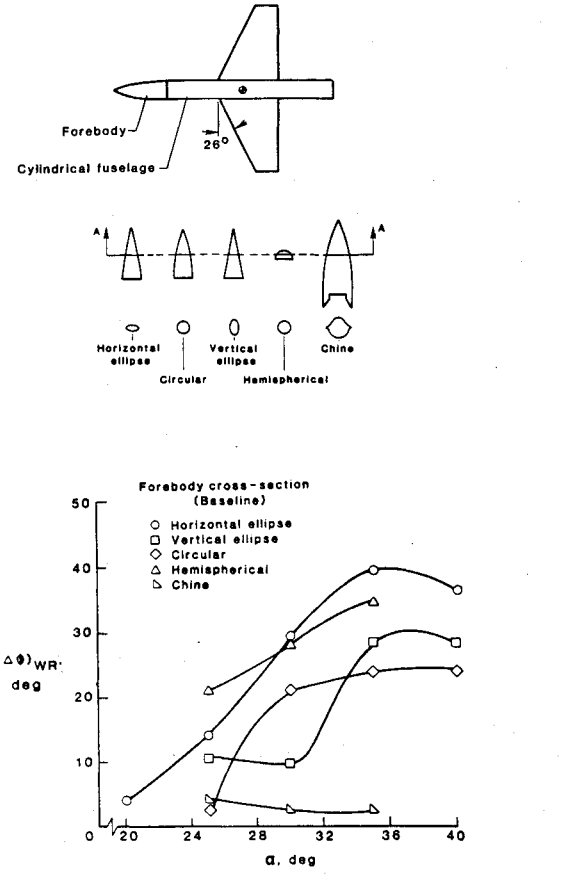


**Fig. 11 Effect on wing-rock amplitude of the cross-sectional shape of a 3-caliber nose (see Ref. 24).**

(Fig. 11). The other geometric shapes had surprisingly similar wing-rock characteristics. The fluid-mechanical reason for this is discussed at length in Ref. 27, where it is also shown that the wing rock is not caused by some interaction between the wing and the asymmetric vortices generated by the nose. The wing simply provides the downstream surfaces needed for generation of the wing-rock driving rolling moment.

### Motion-Induced Asymmetry Switching

Flow mechanisms able to cause a switching of the crossflow separation geometry have been described before.[28] So-called microasymmetries on the nose cause the separation asymmetry and associated side force to vary with body roll angle. At the angles of attack at which steady asymmetric sideforce is generated at zero sideslip, freestream turbulence[29] and support vibration[30] can generate unsteady side-force behavior. However, it is found that even the low angular rates asociated with conventional vehicle maneuvers will dominate over the effects of nose microasymmetries and flow unsteadiness.[31] Classic experiments with rotating circular cylinders illustrate the characteristics of so-called moving-wall effects.

Figure 12 shows experimental Magnus lift results for laminar flow conditions[32] (at $U_W = 0$). Below $U_W/U_\infty = 0.3$, the Magnus lift is generated mainly by the downstream moving-wall effect on the top side, moving the separation from the subcritical toward the supercritical position. On the bottom side, the separation is already of the subcritical type at $U_W = 0$, and the upstream moving-wall effect does not have much leverage for its separation-promoting action. When the rotation rate is increased beyond a critical value, so-called Magnus lift reversal occurs. The critical value of $U_W/U_\infty$ depends on the Reynolds number, being $U_W/U_\infty \approx 0.3$ for the value $Re = 0.128 \times 10^6$. This lift reversal is caused by the moving-wall effect on boundary-layer transition. When $p > p_{crit}$, the up-

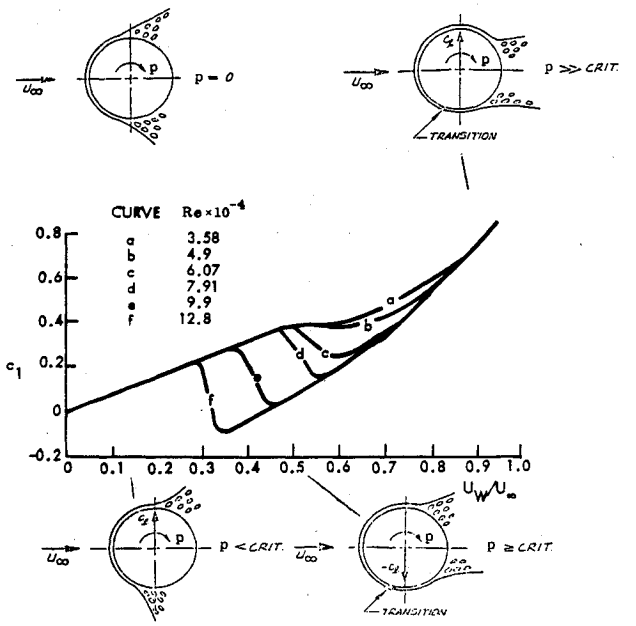


**Fig. 12 Moving-wall effects on a rotating circular cylinder with laminar initial flow conditions.**

stream moving-wall effect on the bottom side causes boundary-layer transition to occur before separation, changing it from the subcritical toward the supercritical type. This effect completely overpowers the regular moving-wall effects on separation and causes a more or less discontinuous loss of lift (see Fig. 12). When the Reynolds number is increased to $0.26\times10^6 \le Re \le 0.325\times10^6$, the critical $U_W/U_\infty$ value approaches zero,[28,32] explaining the very large effect of infinitesimal spin rates for a spinning nose tip.[33,34]

It is shown in Ref. 33 how the moving-wall effects on transition could explain the oscillatory type of coning motion observed in experiments with a flat-face cylinder.[35] Similar moving-wall effects cause an oscillatory spin behavior leading to the observed wing rock in the present case.[24,27] In the test performed by Brandon and Nguyen,[24] the Reynolds number was $0.26\times10^6$. The crossflow over the nose will, therefore, be in the critical Reynolds number region just discussed, providing the following scenario[14] (see Fig. 13). At $t=t_1$, the upstream moving-wall effect causes boundary-layer transition to occur in the forebody crossflow before separation occurs. This changes the flow separation from the subcritical toward the supercritical type. Neglecting time lag effects, the vortex geometry sketched at $t=t_1$ would result. Due to time-lag effects, similar to those discussed in Ref. 27, this vortex geometry (only the lower vortex is shown as only it will induce significant loads on the wing body) is not realized until $t=t_1+\Delta t$. At $t=t_3$, when the roll rate reaches its maximum in the opposite direction, another switch of the separation asymmetry on the forebody occurs. Because of the time-lag effect, the vortex geometry at the (now horizontal) wing has not changed but is the same at $t=t_1+\Delta t$. During the time lag $\Delta t$, the vortex-induced rolling moment drives the rolling motion. That is, the time lag generates negative damping just as in the case of slender wing rock.[8,12]

That the amplitude buildup that is much faster in the case of asymmetric forebody vortices (see Fig. 14) than in the case of asymmetric delta-wing leading-edge vortices (see Fig. 1) can be explained as follows: At some station on the slender nose, the critical flow condition exists for which the transition-induced switch in separation asymmetry will occur for infinitesimally small roll rates. As the amplitude builds up because of the wing-body response, the axial extent over which the transition-induced switch of separation asymmetry can occur grows from half cycle to half cycle of the oscillation.[27,37] The finite extent of this critical flow region is well illustrated by Keener's flow visualization results.[36] This self-feeding flow mechanism can be expected to cause a much faster amplitude buildup than in the case of the slender delta wing, where the vortex strength is essentially unchanged from half cycle to half cycle.

Obviously, the flow mechanism described here, the transition-induced separation reversal, cannot be realized at laminar flow conditions, at least not if the Reynolds number is less than $5.0\times10^4$, as the experimental data[32] in Fig. 12 indicate that no reversal can be generated by moving-wall effects at such a low Reynolds number. On the other hand, when the Reynolds number is increased to $10^6$ or more, the transition-induced reversal can only occur on the slender nose near the apex. Thus, although wing rock can still be generated, it should be less serious.

## Experimental Simulation Difficulties

In view of the fact that all the nonlinear aerodynamic phenomena discussed are generated by separated flow, one has to be greatly concerned about the applicability of subscale test data to full-scale flight conditions.[6,38-40] Comparing the dynamic stall results obtained by Liiva et al.[17] (see Figs. 5 and 14b) with those obtained by Rainey[41] (see Fig. 14a), one gets some appreciation for the difficulties involved when using subscale wing-rock data for a conventional wing. Carta,[42] who made the comparison shown in Fig. 14, obtained test data that agreed with Rainey's data[41] (Fig. 14a). It can be shown[19] that in the case of leading-edge stall, when a significant lift loss occurs, as in Liiva's test,[17] the negative damping in plunge shown in Fig. 8 will occur. However, in Rainey's and Carta's tests,[41,42] the Reynolds number was so low that laminar-type static stall without major lift loss was experienced. This would

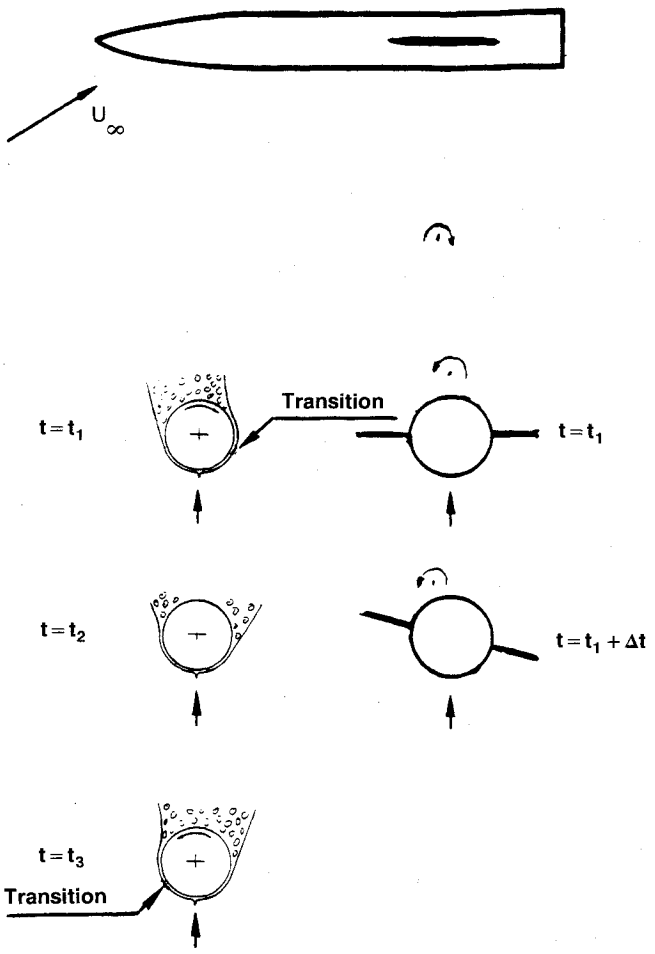


**Fig. 13 Conceptual flow mechanism for wing-body rock (see Ref. 27).**

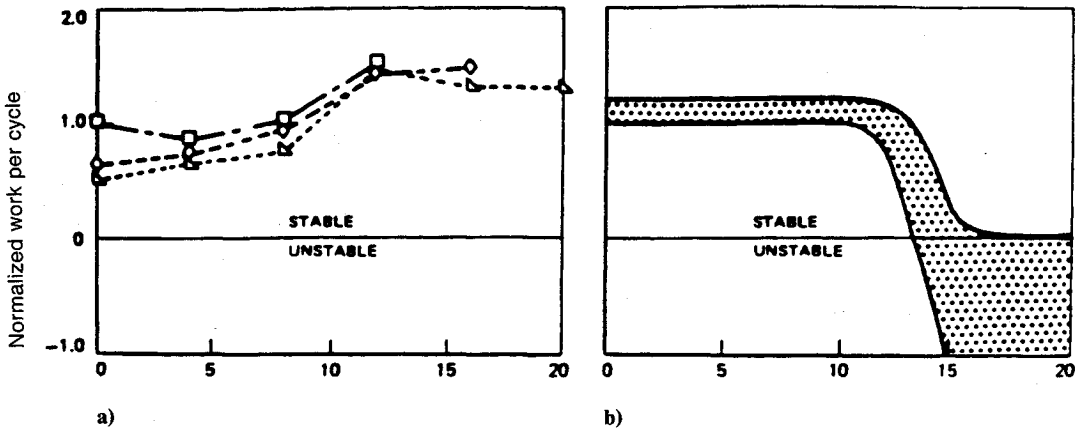


**Fig. 14 Damping characteristics for the NACA-0012 Airfoil in plunging oscillations (see Ref. 42): a) Rainey[41]; and b) Liiva et al.[17]**

explain the absence of negative damping in plunge. However, both Rainey's and Carta's tests showed the damping not only to be positive at stall but to be significantly larger than the attached flow damping. What can be the reason for this abnormal behavior?

It is shown in Refs. 21 and 43 that upstream moving-wall effects on boundary-layer transition, similar to those causing negative Magnus lift on a rotating cylinder,[32] cause the plunging airfoil to have a stall behavior that varies between leading-edge stall and laminar stall in a fashion that will provide the measured high damping values. Thus, wind-tunnel tests of conventional wing rock have to be performed at a Reynolds number high enough to give the same stall type as in the full-scale flight. In that case "analytic extrapolation" is possible from the subscale test data to full-scale vehicle dynamics.[44]

For a slender wing with rounded leading edges one would expect to find moving-wall effects similar to those just discussed for the straight or moderately swept wing. However, analysis of experimental pitch damping results for slender delta wings[45,46] reveals that they are absent and that the dynamic flow conditions at apex and the delay of static stall due to leading-edge roundness are the controlling factors. Reynolds number effects, however, can become significant for slender wings in general, even when the leading edge is sharp, through their influence on the secondary flow separation of the outflow toward the leading edge,[47,48] which in turn will affect the primary separation behavior.

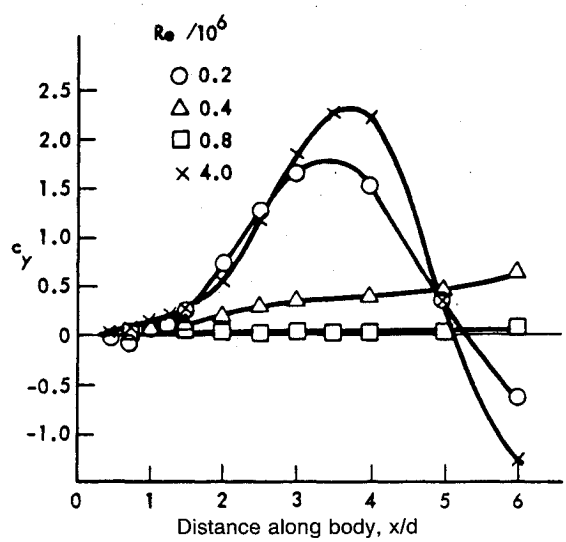


**Fig. 15 Effect of Reynolds number on the side-force distribution on an ogive-cylinder body (see Ref. 49).**

The asymmetric vortex shedding from a slender nose is very sensitive to Reynolds number as well as to turbulence and roughness, as can be appreciated from the flow pictures in Ref. 36 and the measured side-force distribution on a pointed ogive-cylinder body[49] (see Fig. 15). The fluid mechanical reasons for the large effect of Reynolds number demonstrated by the results in Fig. 15 are discussed in detail in Ref. 50. A complete review of the transition effects on dynamic simulation is given in Ref. 51.

## Conclusions

An analysis of available experimental data for aircraft configurations at high angles of attack reveals that wing rock can be generated by three different fluid mechanical flow processes.

1) Slender wing rock is caused by asymmetric leading-edge vortices, and vortex burst is the flow mechanism limiting the growth of the wing-rock amplitude.

2) Conventional wing rock of aircraft wings with straight or moderately swept leading edges is caused by negative damping in plunge of airfoil sections experiencing leading-edge-type stall with associated significant lift loss.

3) Wing-body rock is caused by asymmetric vortex shedding from a slender forebody, where moving wall effects cause a transition-induced reversal of the separation asymmetry and associated vortex asymmetry. Downstream wing and/or tail surfaces do not interact directly with the asymmetry-generating flow mechanism. They only provide the means whereby the asymmetric body vortices can generate the wing-rock-driving rolling moment.

At the present, the highly nonlinear aerodynamics causing the above vehicle motions can in general only be defined experimentally, a task complicated greatly by various types of simulation difficulties in subscale testing.

## References

[1]"Dynamic Stability Parameters," AGARD CP-235, Nov. 1978.

[2]Ericsson, L. E., "Technical Evaluation Report on the Fluid Dynamics Panel Symposium on Dynamic Stability Parameters," AGARD-AR-137, April 1979.

[3]Ericsson, L. E., "A Summary of AGARD FDP Meeting on Dynamic Stability Parameters," AGARD CP-260, Paper 2, May 1979.

[4]Orlik-Rückemann, K. J., "Dynamic Stability Testing of Aircraft-Needs Versus Capabilities," *Progress Aerospace Sciences*, Pergamon, New York, 1975.

[5]Ericsson, L. E., and Reding, J. P., "Review of Support Interference in Dynamic Tests" *AIAA Journal*, Vol. 21, No. 12, 1983, pp. 1652–1666.

[6]Ericsson, L. E., and Reding, J. P., "Scaling Problems in Dynamic Tests of Aircraft-Like Configurations," AGARD-CP-227, Paper 25, Sept. 1977.

[7]Nguyen, L. T., Yip, L. P., and Chambers, J. R., "Self-Induced

Wing Rock of Slender Delta Wings," AIAA Paper 81-1883, Aug. 1981.

[8]Ericsson, L. E., "The Fluid Mechanics of Slender Wing Rock," *Journal of Aircraft*, Vol. 21, No. 5, 1984, pp. 322-328.

[9]Ericsson, L. E., "Unsteady Aerodynamics of Separating and Reattaching Flow on Bodies of Revolution," *Recent Research on Unsteady Boundary Layers*, Vol. 1, IUTAM Symposium, Laval Univ., Quebec, May 1971, pp. 575-586.

[10]Polhamus, E. C., "Predictions of Vortex-Lift Characteristics by a Leading-Edge Suction Analogy," *Journal of Aircraft*, Vol. 8, 1971, pp. 193-199.

[11]Lambourne, N. C., Bryer, D. W., and Maybrey, J. F. M., "The Behavior of the Leading-Edge Vortices over a Delta Wing Following a Sudden Change of Incidence," Aeronautical Research Council, Great Britain, R&M No. 3645, March 1969.

[12]Ericsson, L. E., "Analytic Prediction of the Maximum Amplitude of Slender Wing Rock," *Journal of Aircraft*, Vol. 26, No. 1, 1989, pp. 35-39.

[13]Wendtz, W. H., and Kohlman, D. L., "Vortex Breakdown on Slender Sharp-Edged Delta Wings," AIAA Paper 69-778, July 1969.

[14]Konstadinapoulus, P., Mook, D. T., and Nayfeh, A. H., "Numerical Simulation of the Subsonic Wing Rock Phenomenon," AIAA Paper 83-2115, Aug. 1983.

[15]Konstadinopoulus, P., Mook, D. T., and Nayfeh, A. H., "Subsonic Wing Rock of Slender Delta Wings," *Journal of Aircraft*, Vol. 22, No. 3, 1985, pp. 223-228.

[16]Katz, J., and Levin, D., "Self-Induced Roll Oscillations Measured on a Delta Wing/Canard Configuration," *Journal of Aircraft*, Vol. 23, 1986, pp. 801-807.

[17]Liiva, J., Davenport, F. J., Gray, L., and Walton, I. C., "Two-Dimensional Tests of Airfoils Oscillating Near Stall," U.S. Army Aviation Labs, Fort Eustis, VA, TR 68-13, April 1968.

[18]Ericsson, L. E., and Reding, J. P., "Stall Flutter Analysis," *Journal of Aircraft*, Vol. 10, No. 1, 1973, pp. 5-13.

[19]Ericsson, L. E., and Reding, J. P., "Dynamic Stall Analysis in Light of Recent Numerical and Experimental Results," *Journal of Aircraft*, Vol. 13, No. 4, 1976, pp. 248-255.

[20]Mabey, D. G., Ashill, P. R., and Welsh, B. L., "Aeroelastic Oscillations Caused by Transitional Boundary Layers and Their Attenuation," *Journal of Aircraft*, Vol. 24, No. 7, 1987, pp. 463-469.

[21]Ericsson, L. E., "Transition Effects on Airfoil Dynamics and the Implication for Subscale Tests," *Journal of Aircraft* Vol. 26, No. 12, 1989, pp. 1051-1058.

[22]den Boer, R. G., and Houvink, R., "Analysis of Transonic Aerodynamic Characteristics for a Supercritical Airfoil Oscillating in Heave, Pitch and with Oscillating Flap," AGARD CP-374, Paper 4, Jan. 1985.

[23]Fratello, D. J., Croom, M. A., Nguyen, L. T., and Domack, C. S., "Use of the Updated NASA Langley Radio-Controlled Drop-Model Technique for High-Alpha Studies of the X-29A Configuration," AIAA Paper 87-2559, Aug. 1987.

[24]Brandon, J. M., and Nguyen, L. T., "Experimental Study of Effects of Forebody Geometry on High Angle of Attack Stability," *Journal of Aircraft*, Vol. 25, No. 7, 1988, pp. 591-597.

[25]Ericsson, L. E., and Reding, J. P., "Review of Vortex-Induced Asymmetric Loads—Part I," *Z. Flugwiss. Weltraumforsch*, Vol. 5, No. 3, 1981, pp. 162-174.

[26]Ericsson, L. E., and Reding, J. P., "Review of Vortex-Induced Asymmetric Loads—Part II," *Z. Flugwiss. Weltramforsch.*, Vol. 5, No. 6, 1981, pp. 849-866.

[27]Ericsson, L. E., "Wing Rock Generated by Forebody Vortices," *Journal of Aircraft*, Vol. 26, No. 2, 1989, pp. 110-116.

[28]Ericsson, L. E., and Reding, J. P., "Asymmetric Vortex Shedding from Bodies of Revolution," *Tactical Missile Aerodynamics, Progress in Astronautics and Aeronautics,* edited by M. J. Hemsch and J. N. Nielsen, Vol. 104, 1986, pp. 243-296.

[29]Ericsson, L. E., and Reding, J. P., "Vortex Unsteadiness on Slender Bodies at High Incidence," *Journal of Spacecraft and Rockets*, Vol. 24, No. 4, 1987, pp. 319-326.

[30]Ericsson, L. E., "Lateral Oscillations of Sting-Mounted Models at High Alpha," AIAA Paper 89-0047, Jan. 1989.

[31]Ericsson, L. E., "Moving Wall Effects in Unsteady Flow," *Journal of Aircraft*, Vol. 25, No. 11, 1988, pp. 977-990.

[32]Swanson, W. M., "The Magnus Effect: A Summary of Investigations to Date," *Journal of Basic Engineering*, Vol. 83, Sept. 1961, pp. 461-470.

[33]Ericsson, L. E., and Reding, J. P., "Dynamics of Forebody Flow Separation and Associated Vortices," *Journal of Aircraft*, Vol. 22, No. 4, 1985, pp. 329-335.

[34]Fidler, J. E., "Active Control of Asymmetric Vortex Effects," *Journal of Aircraft*, Vol. 18, No. 4, 1981, pp. 267-272.

[35]Yoshinaga, T., Tate, A., and Inoue, K., "Coning Motion of Slender Bodies at High Angles of Attack in Low Speed Flow," AIAA Paper 81-1899, Aug. 1981.

[36]Keener, E. R., "Flow-Separation Patterns on Symmetric Forebodies," NASA TM-86016, Jan. 1986.

[37]Ericsson, L. E., "Further Analysis of Wing Rock Generated by Forebody Vortices," *Journal of Aircraft,* Vol. 26, No. 12, 1989, pp. 1098-1104.

[38]Ericsson, L. E., and Reding, J. P., "Reynolds Number Criticality in Dynamic Tests," AIAA Paper 78-166, Jan. 1978.

[39]Ericsson, L. E., and Reding, J. P., "Practical Solutions to Simulation Difficulties in Subscale Wind Tunnel Tests," AGARD-CP-348, Paper 16, Sept. 1983.

[40]Ericsson, L. E., "Reflections Regarding Recent Rotary Rig Results," *Journal of Aircraft*, Vol. 24, No. 1, 1987, pp. 25-30.

[41]Rainey, A. G., "Measurement of Aerodynamic Forces for Various Mean Angles of Attack on an Airfoil Oscillating in Bending with Emphasis on Damping in Stall," NACA Rept. 1305, 1957.

[42]Carta, F. O., "A Comparison of the Pitching and Plunging Response of an Oscillating Airfoil," NASA CR 3172, Oct. 1979.

[43]Ericsson, L. E., and Reding, J. P., "The Difference Between the Effects of Pitch and Plunge on Dynamic Airfoil Stall," *Ninth European Rotorcraft Forum*, Paper No. 8, Sept. 1983.

[44]Ericsson, L. E., and Reding, J. P., "Analytic Extrapolation to Full Scale Aircraft Dynamics," *Journal of Aircraft*, Vol. 21, No. 3, 1984, pp. 222-223.

[45]Ericsson, L. E., and Reding, J. P., "Unsteady Aerodynamics of Slender Delta Wings at Large Angles of Attack,"*Journal of Aircraft*, Vol. 12, No. 9, 1975, pp. 721-729.

[46]Ericsson, L. E., and Reding, J. P., "Approximate Nonlinear Slender Wing Aerodynamics," *Journal of Aircraft*, Vol. 14, No. 12, 1977, pp. 1197-1204.

[47]Hummel, D., "Experimentelle Untersuchung der Strömung auf der Saugseite eines Schlanken Deltaflügels," *Z. Flugwiss*, Vol. 13, No. 7, 1965, pp. 247-252.

[48]Ericsson, L. E., "What About Transition Effects?" AIAA Paper 88-0564, (see Appendix), Jan. 1988.

[49]Lamont, P. J., "Pressures Around an Inclined Ogive-Cylinder With Laminar, Transitional, and Turbulent Separation," *AIAA Journal*, Vol. 20, Nov. 11, 1982, pp. 1492-1499.

[50]Reding, J. P., and Ericsson, L. E., "A Re-examination of the Maximum Normalized Vortex-Induced Side Force," *Journal of Spacecraft and Rockets*, Vol. 21, No. 5, 1984, pp. 433-440.

[51]Ericsson, L. E., "Review of Transition Effects on the Problem of Dynamic Simulation," AIAA Paper 88-2004, May 1988.